

Turbulent Diffusion and Mixing in non-homogeneous Environments

**Jose M. Redondo (1,2), Margarita Diez (1,3),
Emil Sekula (1) and Otman Ben Mahjoub (1,4)**

- (1) Universitat Politecnica de Catalunya (UPC), Dept. Fisica Aplicada, Barcelona, 08034, Spain (redondo@fa.upc.edu, +34-(0)934016090),,
(2) Pan European Laboratory on non-homogeneous Turbulence, LAB-ERCOFTAC,
(3) Port GenCat. CUM, Vilanova i la Geltru, 08800 Spain
(4) Instituto PluriDisciplinar, U.C.M. ERCOFTAC. Madrid, Spain

Many experimental and field studies have been devoted to the understanding of non-homogeneous turbulent dynamics. Activity in this area intensified when the basic Kolmogorov self-similar theory was extended to two-dimensional or quasi 2D turbulent flows such as those appearing in the environment, that seem to control mixing [1,2]. The statistical description and the dynamics of these geophysical flows depend strongly on the distribution of long lived organized (coherent) structures. These flows show a complex topology, but may be subdivided in terms of strongly elliptical domains (high vorticity regions), strong hyperbolic domains (deformation cells with high energy condensations) and the background turbulent field of moderate elliptic and hyperbolic characteristics. It is of fundamental importance to investigate the different influence of these topological diverse regions.

Relevant geometrical information of different areas is also given by the maximum fractal dimension, which is related to the energy spectrum of the flow. Using all the available information it is possible to investigate the spatial variability of the horizontal eddy diffusivity $K(x,y)$. This information would be very important when trying to model numerically the behaviour in time of the oil spills [3,4] There is a strong dependence of horizontal eddy diffusivities with the Wave Reynolds number as well as with the wind stress measured as the friction velocity from wind profiles measured at the coastline.

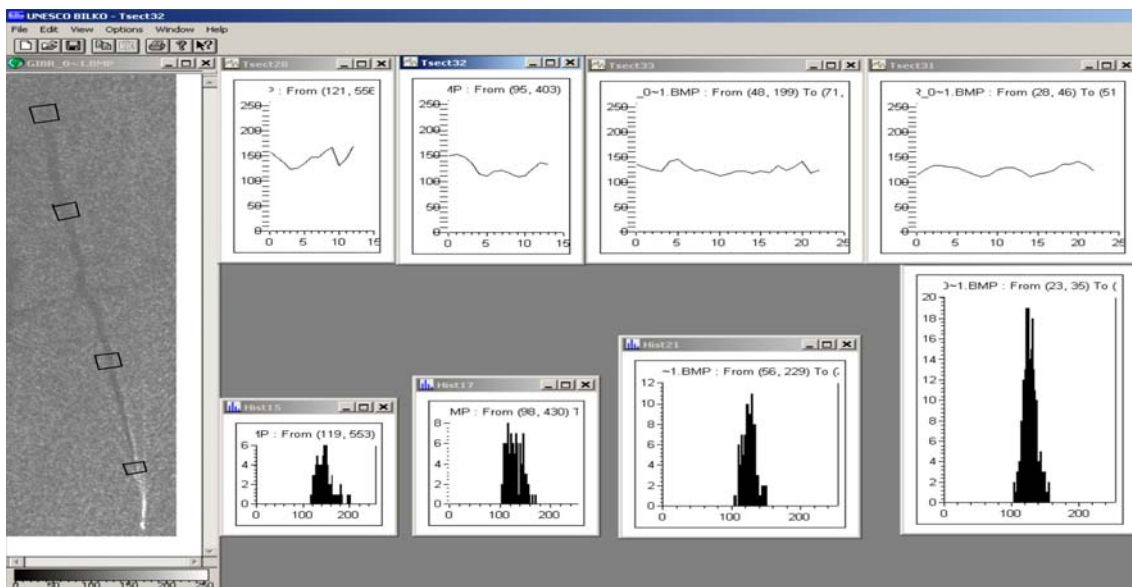
Natural sea surface oily slicks of diverse origin (plankton, algae or natural emissions and seeps of oil) form complicated structures in the sea surface due to the effects of both multiscale turbulence and Langmuir circulation. It is then possible to use the topological and scaling analysis to discriminate the different physical sea surface processes.

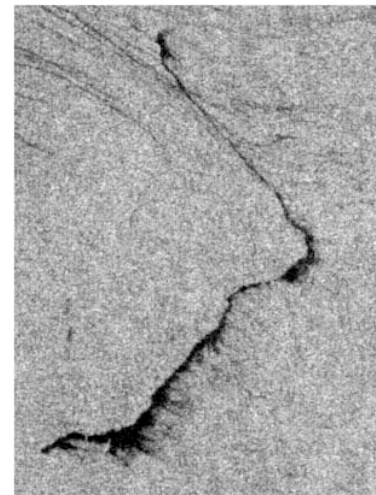
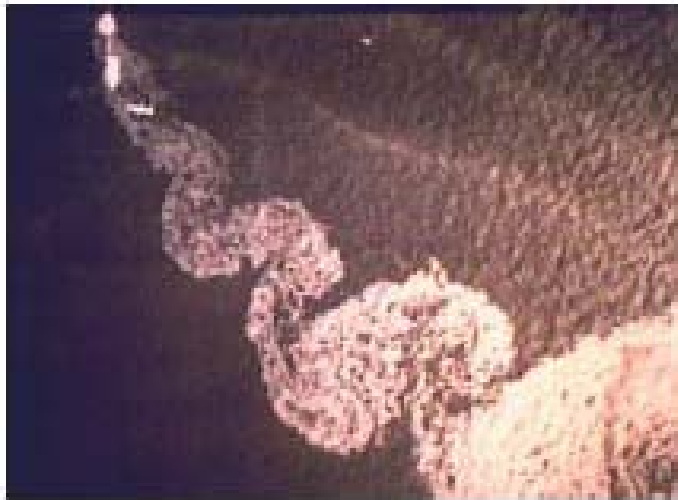
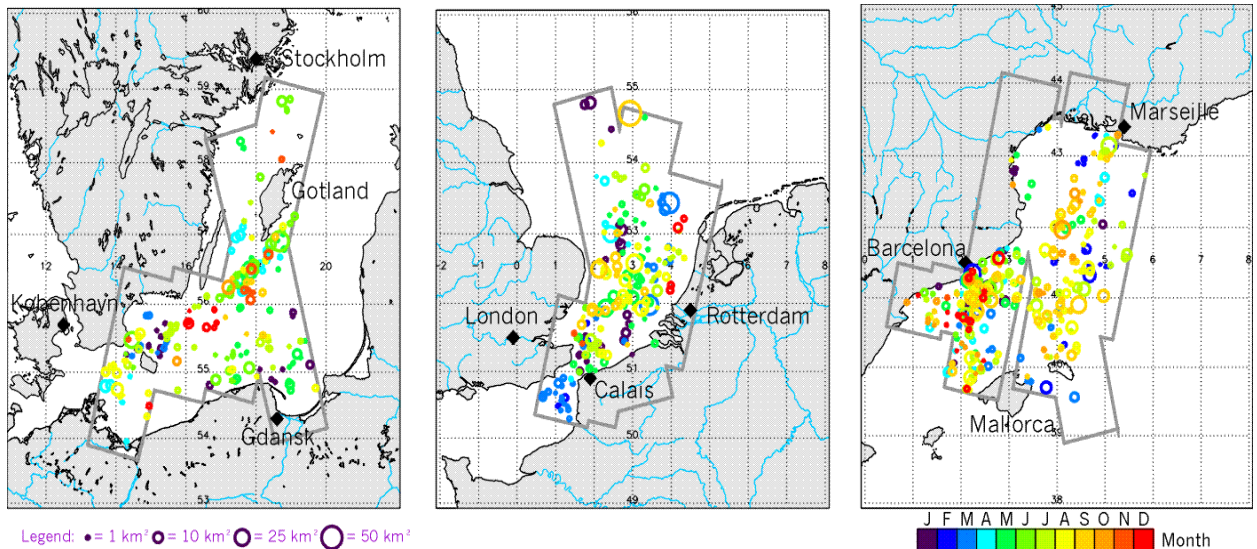
We can relate higher order moments of the Lagrangian velocity to effective diffusivity in spite of the need to calibrate the different regions determining the distribution of mesoscale vortices and other dominant features [5,2].

We present relationships used to parameterise the sub-grid turbulence in terms of generalized diffusivities that take into account the topology and the self-similarity of the sea surface environment.

Multifractal analysis can also be used to distinguish fresh oil spills and natural slicks in the ocean surface, with residence time the difference diminishes (The Damkohler number scales the time with rough weather accelerating the dilution). Modelling the Rossby deformation scale dynamics is fundamental to predict oil spill behaviour as this range is the most energetic.

The geometric and topological features of the interaction between the spectral and multi-fractal structure of the fronts driven by acceleration induced instabilities RT as well as of different wakes have been investigated following ImaCalc Fractal box-counting algorithm for the different sets of different intensity and marked value ranges, Grau(2005). Further analysis on Mixing experiments with a similar set up as in Linden and Redondo(1991) have been used to relate multifractal and spectral measurements of the density, velocity and vorticity fields as they evolve, the volume fraction and the mixing products is also detected with chemical reactive and non reactive tracers.





The methodology that relates a generalized intermittency (Mahjoub et al 1998) and anomalous scaling while mixing is taking place is used to evaluate scalar and tracer diffusivity and it is applied both in the RT mixing fronts as well as in other complex flows (Diez et al (2008), Vila et al(2011), Layzet et al. (2008,2010)). The regions of localized mixing, have a higher range of multifractal dimension values, and using box-counting and wavelet analysis, where the turbulent cascade reaches the Batchelor scales indicates the statistical structure of the instability driven mixing process. (**Fig. 1.**)

It is important to measure diffusivity and mixing efficiency, specially when non homogeneous turbulence is produced by one or several body forces like buoyancy, rotation or magnetic fields. The role of internal and inertial waves seems to affect the locality of the cascade processes. Arquimedes and Coriolis forces produce changes in the scaling (Redondo et al 1996, 2003, 2008) which is related to the local Richardson, Ri , Reynolds and inverse Rossby, $1/Ro$ numbers is used to identify the dominant mixing instabilities and the changes in spectra and intermittency

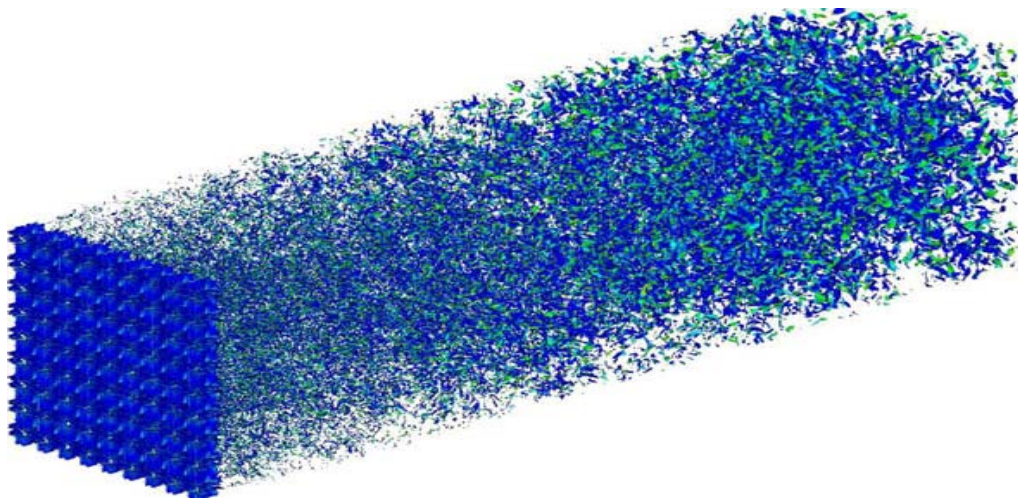


Fig 1. Visualization of a turbulent grid wake (Layzet et al 2008-2010)

Most of the mixing taking place in the sides of the coherent structures, i.e. blobs and spikes. The use of LES simulations and of KS synthetic turbulence is compared as reported by Redondo and Garzon (2004), Redondo et al.(2006) where numerical simulations agree with the experiments and gives further insight on the different cascading processes that take place in the flow, mainly the tracer density spectra, the velocity, the vorticity spectra and the multi-fractal evolution.

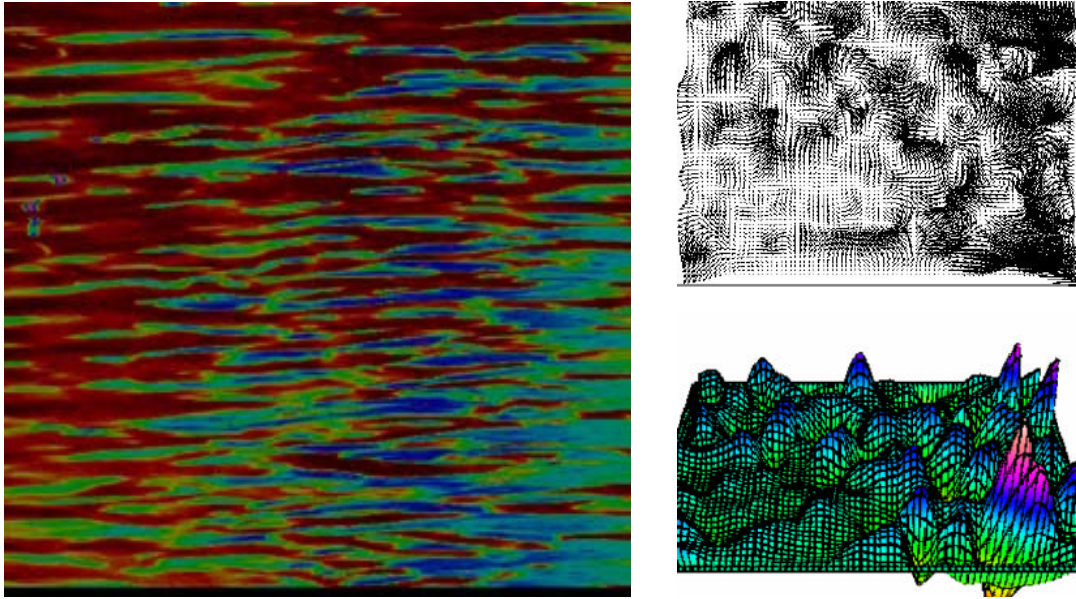


Fig 2. Visualization of a density interface in a stratified zero-mean flow

Mixing efficiency is estimated locally, both in time and space relating the maximum fractal dimension of the velocity and volume fraction sets and comparing the LES and the experiments.

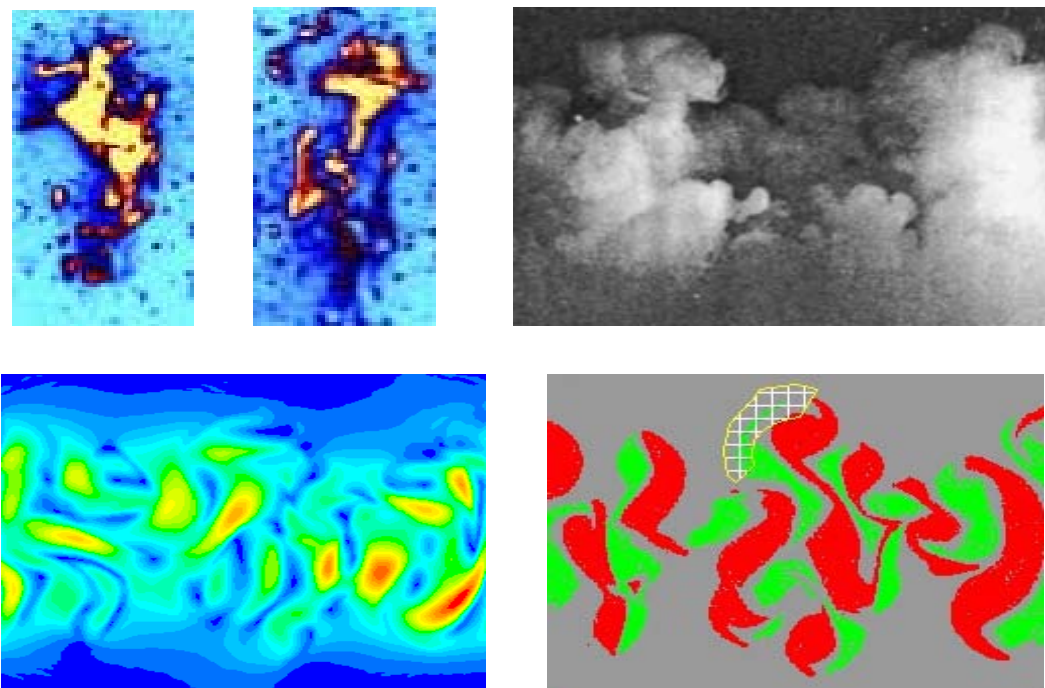


Fig 3. Visualization of a Rayleigh Taylor Experiment and LES simulation

Overall mixing efficiency and the evolution of local mixing efficiency are compared for a set of low Atwood number

experiments and LES simulations of the Rayleigh-Taylor instability (**Fig 3.**). The differences between the acceleration of the RT fronts, pressure shock induced compressible RM fronts and rotating-stratified interacting vortices, have different topologies and produce very different local and global mixing descriptors, probably because of the cascade asymmetry and intermittency, these effects and the evaluation of diffusion are also discussed with environmental and geophysical applications in mind.

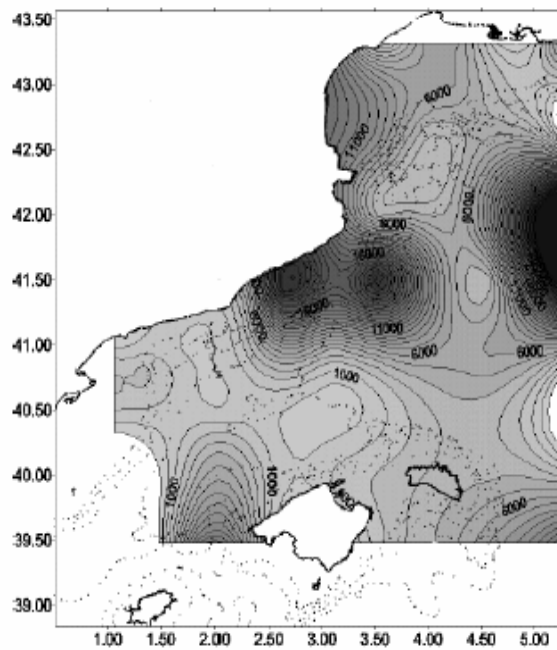
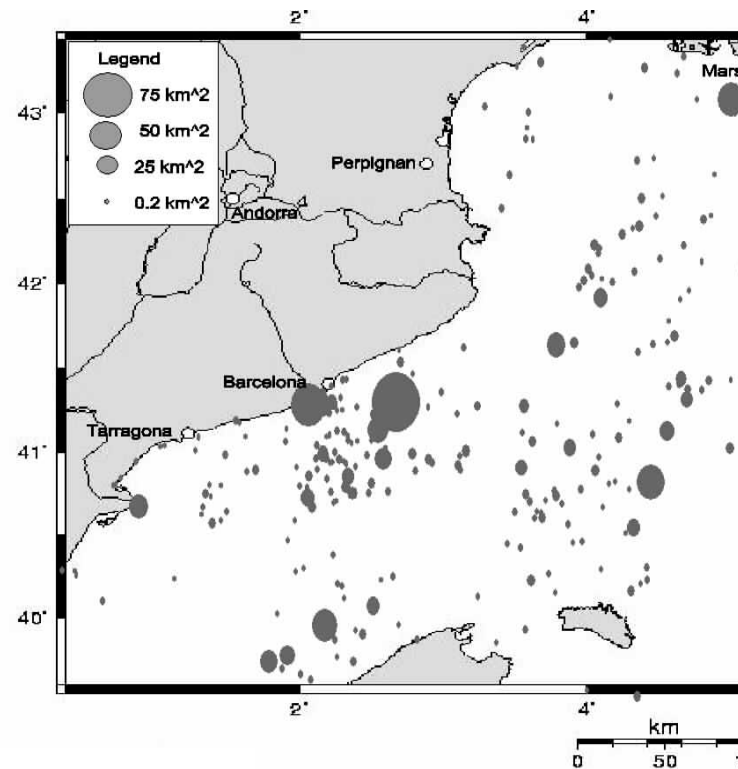
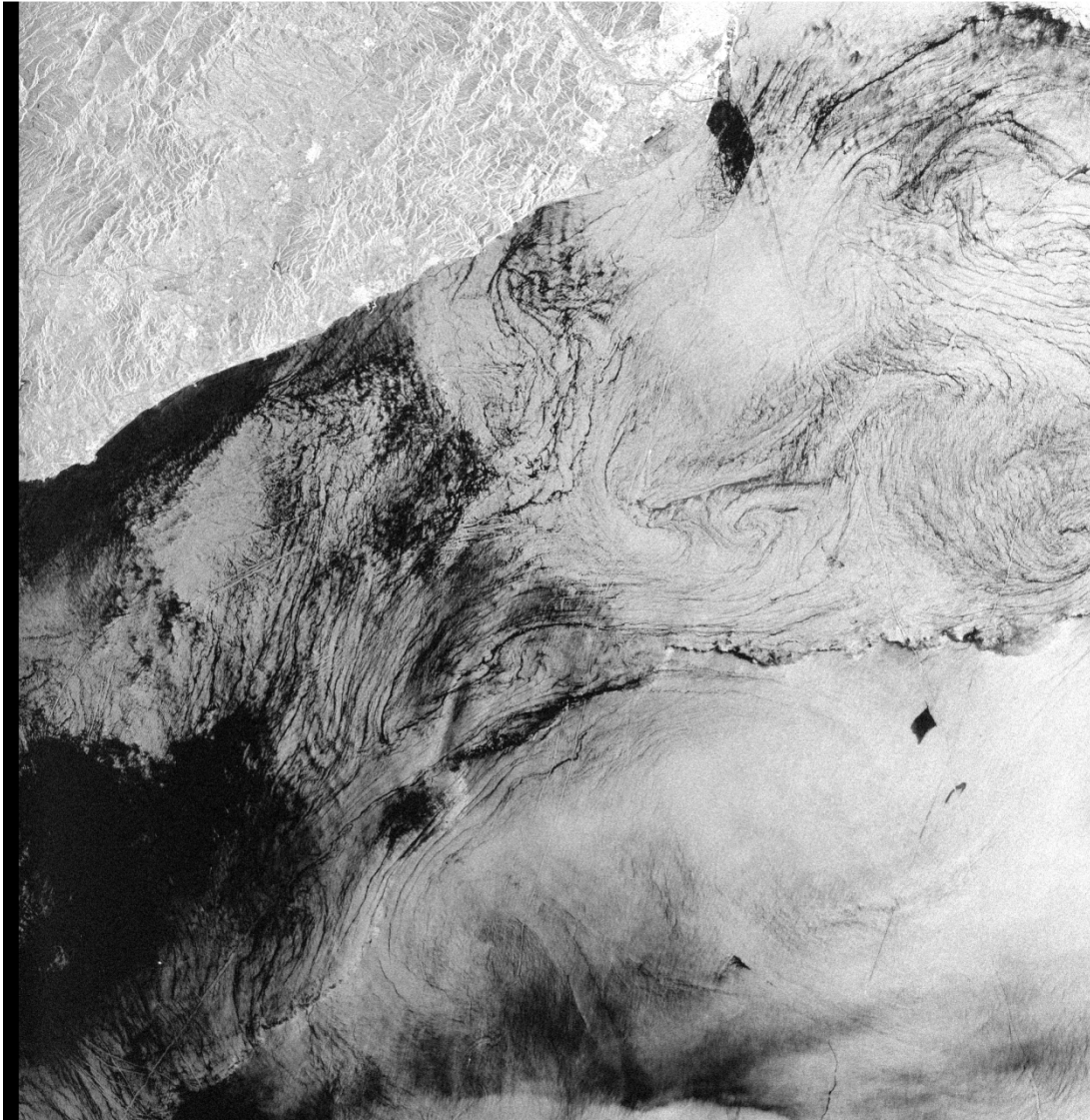


Figure 6. Map of Averaged horizontal eddy diffusivity of the Gulf of Li area obtained by SAR analysis during 1997 and 1998. X is Longitude and Latitude. The Eddy diffusivity average values are in (m^2s^{-1}) calcula according to Richardson's 4/3 law for a 10 km spill.

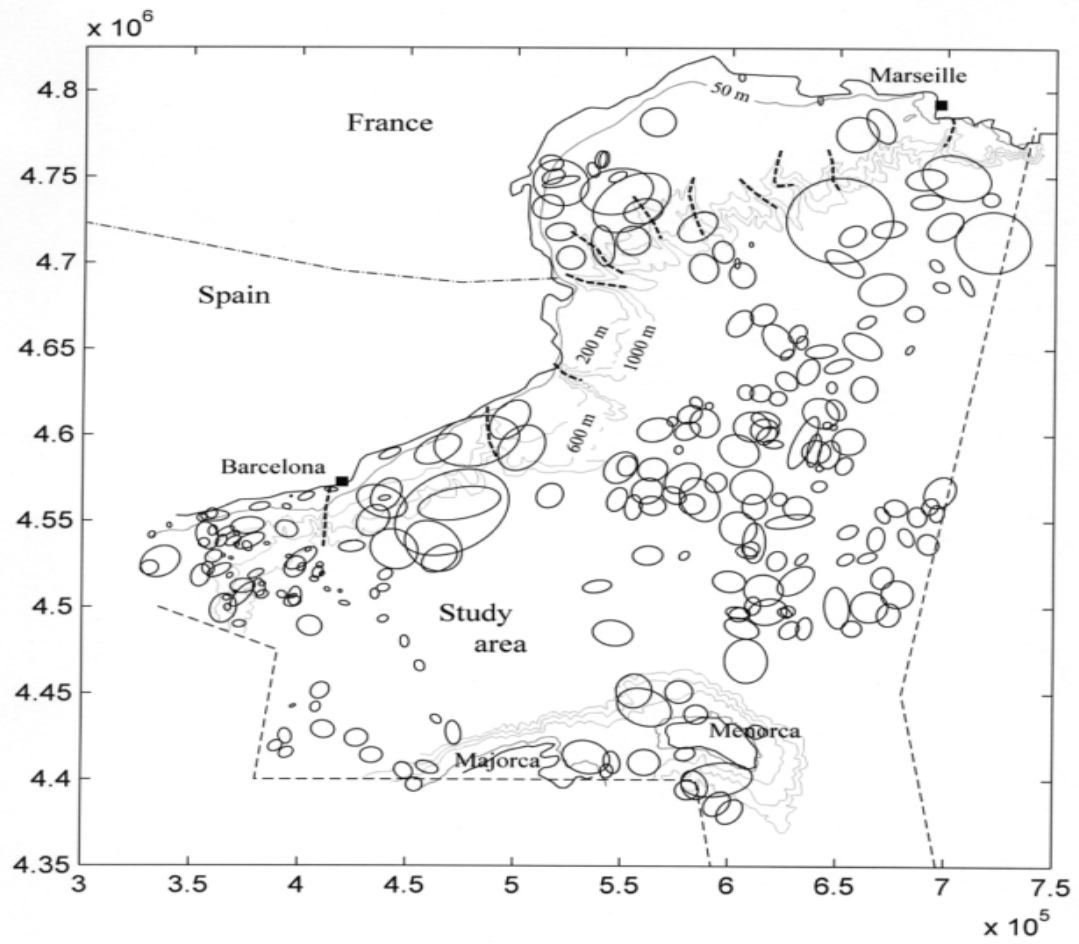


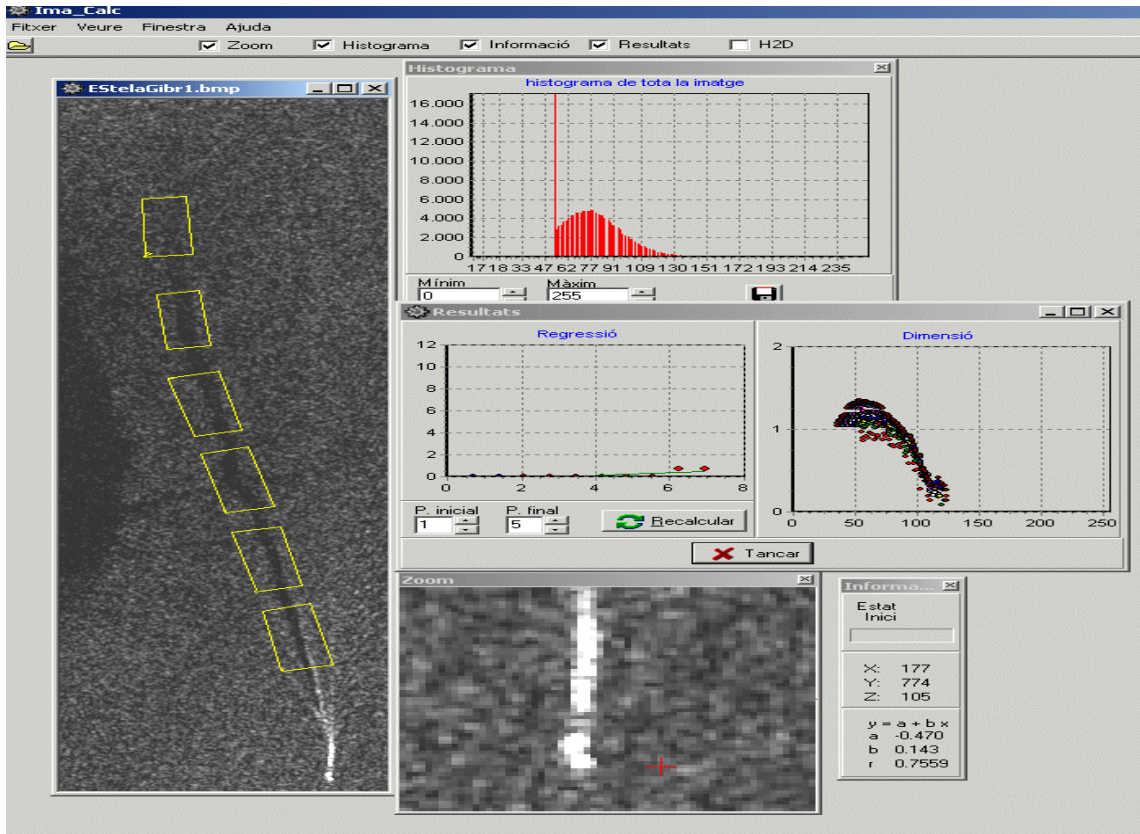
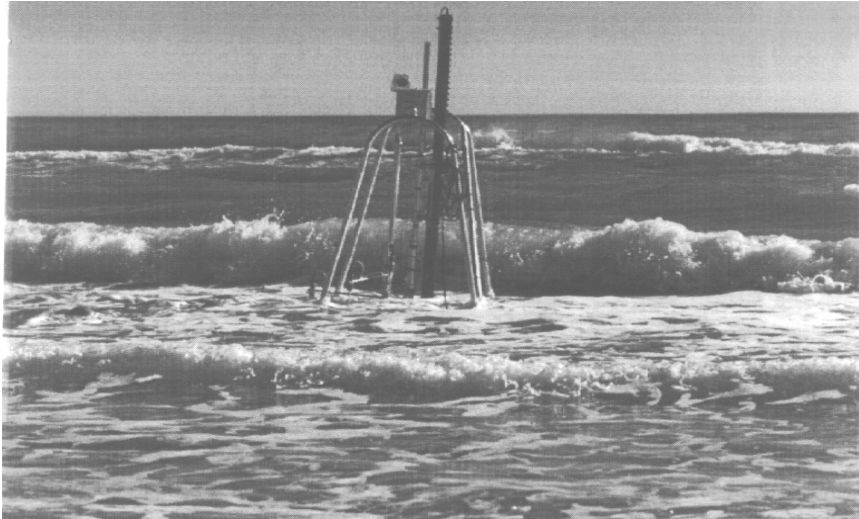
Detected oil patches during 1996 - 1998 in the NW Mediterranean by means of SAR observations.

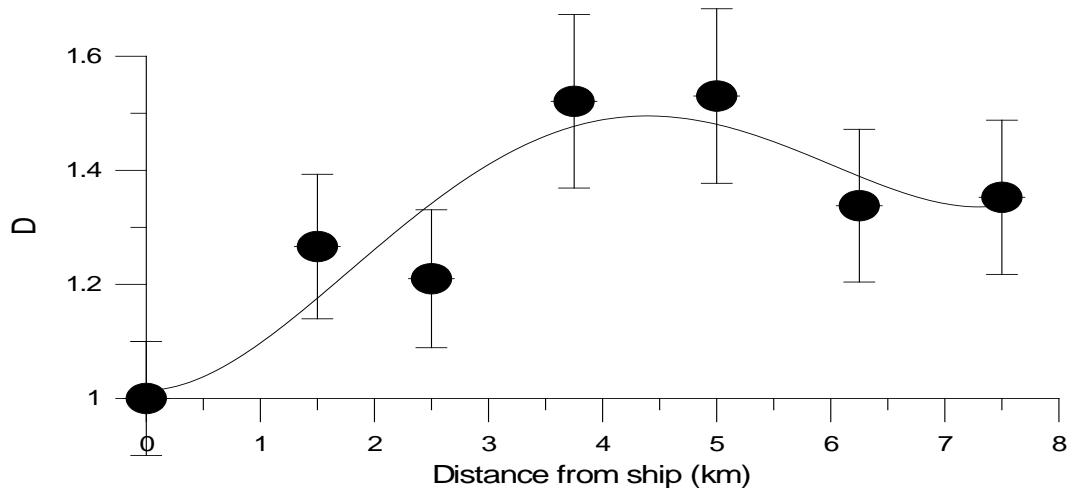


Relevant geometrical information of different areas is also given by the maximum fractal dimension, which is related to the energy spectrum of the flow. Using all the available information it is possible to investigate the spatial variability of the horizontal eddy diffusivity $K(x,y)$. This information would be very important when trying to model numerically the behaviour in time of the oil spills

There is a strong dependence of horizontal eddy diffusivities with the Wave Reynolds number as well as with the wind stress measured as the friction velocity from wind profiles measured at the coastline. Some of these results have been published in Bezerra et al. (1998).







The theory and applications of fractal analysis is a rapidly evolving research field both from a mathematical approach and in experimental and field applications. The basic theory and method of box-counting used in ImaCalc tool (Grau, 2005) was followed and we used self-similarity to identify different dynamic processes that might influence the radar back-scattering from the ocean surface. The image analysis algorithms are able to detect the selfsimilar characteristics for different SAR intensity levels, i .

The fractal dimension $D(i)$ is then a function of intensity and may be calculated using the box counting algorithm

$$D = \log N(i) / \log e$$

where $N(i)$ is the number of boxes of size e needed to cover the SAR contour of intensity i . The algorithm operates dividing the surface into smaller and smaller square boxes and counting the number of them which have values close to the SAR radiation level under study. Let us assume a convoluted line, which is embedded in a plane (that is why it is usually referred to as $D=2$, or fractal dimension within an Euclidean plane of dimension 2). If it is a single Euclidean line, its (nonfractal) dimension will be one. If it fills the plane its dimension will be two. The boxcounting algorithm divides the embedding Euclidean plane in smaller and smaller boxes (e.g., by dividing the initial length LO by n , which is the recurrence level of the iteration). For each box of size LO/n it is then decided if the convoluted line, which is analysed, is intersecting that box. The number $N(i)$ is the number of boxes which were intersected by the convoluted line (at intensity level i). Finally, we plot N versus LO/n (i.e., the size of the box e) in a loglog plot, and the slope of that curve, within reasonable experimental limits, gives the fractal dimension. Note that the sign of the fractal dimension is not relevant. This is performed for different contour levels corresponding to different SAR intensity

The multifractal analysis of the different backscattered intensity levels in SAR imagery can be used to distinguish between natural and man-made sea surface features due to their distinct selfsimilar properties.

The differences are detected using the multi-fractal box counting algorithm on different sets of SAR images giving also information on the age of the spills.

Recent man-made oil spills in the sea surface are characterized by the low fractal dimension values ($D < 1.2$) over the region of low reflectivity in SAR images, on the other hand natural oil slicks show a typical parabolic shape with maximum of $D \gg 1.4$.

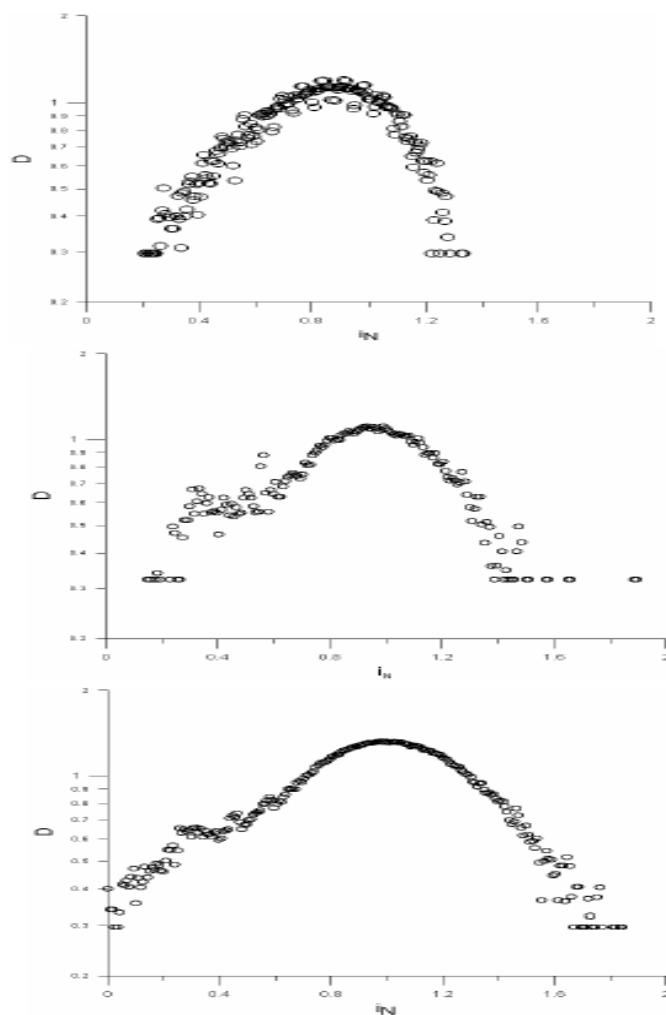


Figure 11. Multi-fractal analysis at a fixed grouping of 3 intensity levels of (above) a natural slick as shown in figure 7 and (below) the marked areas for the two oil spills of figure 9 adrift during different times and diffused in the ocean surface (a logarithmic scale is used).

The comparative statistical analysis of both the 39 years' time tankers known shipwrecks in European coastal waters and the relatively small but common spills shows a power relation between the number of spills and their respective sizes over a seven decade interval. In the logarithmic scale this relation shows a good approximation to Zipf's law (law of increase of entropy) (Zipf, 1949). This basic law is simply described as $i f_i = C$, where i is the event rank, f_i is the frequency of its occurrence and C is a constant), or

$$f_i \approx C i^{-a} \quad (2)$$

In our case f_i is the number of cases of the detection of the oil spills of a certain area rank and i is (the rank or complexity or size of the event (in our case, it is the average area of the spills). The exponent a is a power, whose value is 1 if the described process is independent of the scale. Transforming equation (2) to a logarithmic scale, we obtain:

$$\log f_i = \log C - a \log(i) \quad (3)$$

which is described as a line of slope $-a$ and intercept b .

$$y = b - ax \quad (4)$$

where now x is $\log(i)$, y is $\log f_i$ and $\log C$ is the constant b .

Table The exponent a and coefficient of determination R -squared of equation 4 for the small spills considering different persistence times together with the large accidental spills of figure

Persistence of small oil spills (days)	- a	R
2	-1.077913429	0.989586
3	-1.041143478	0.989522
4	-1.014636617	0.989362
5	-0.994257447	0.989154
6	-0.9770941452	0.988919
7	-0.9635402605	0.988691
variable persistence	-1.132997351	0.982306

The Figure shows the average annual number of small spills (more than 0.1 Km² and less than 75 Km²) for different persistences on the sea surface and at the same time the average annual probability of great spills of more than 35.000 Km². The data is plotted as a

function of their respective areas, both for small and large oil spills occurred in European coastal waters according to tables 4. Also in figure 10 a spatial-temporary normalization of the data sets with different scales was considered. The crude spills' persistence time period is related to many environmental factors, such as surge, wind and dominant current structure. Therefore the probability of detecting the real number of spills with just one observation every 35 days will strongly depend on the environmental conditions and a low persistence will hamper the possibility of detection.

According to the table, the coefficient $-a$ varies between $-1,08$ (2 days' persistence of spills) and $-0,96$ (7 days' persistence). The best fit for both small and large spills corresponds to a 5 day average persistence, as seen in Figure 10, which adjusts better to the Zipf's law distribution (coefficient $a = 0.994$, i.e. close to 1).

The Zipf's law (Zipf, 1949, Mandelbrot 1977) indicates that the frequency of the occurrence of some events associated with the human activities is larger at small scales than at big scales. The function that fits well this rank – frequency dependency has a hyperbolic form (which in a logarithmic scale depicts a straight line with slope -1). This law is almost universal and takes place in linguistic sciences as noted first by (Zipf, 1949) (the frequency of the occurrence of the words with less letters is larger than that of the long words in any language), in social statistics (the number of cities versus their population; Gabaix, 1999; Reed, 2002), in ecology (the biomass of insects versus whales, the biological objects' size distribution (Camacho and Sole, 2001; Reed et al., 2002)), in geophysics ([Sornette et al., 1996](#)) etc. Also it is used to new communication technologies, for example, into Internet's facilities (the automatic index of thematic texts by key words (Popov, 1998) or in web access statistics (Breslau et al., 2000)). Mandelbrot(1977) generalized the law in terms of two fractal dimensions when analysing clustering of islands of fractal contours or in aggregation of events, if D is the fractal dimension of the clustering and D_c that of the basic process, then:

$$a = D_c/D \tag{5}$$

when both processes are uniform then $D_c=D$ and Zipf's law is recovered $f_i = C / i$

In our case, Zipf's law application to the distribution of oil spills according to their sizes allows the following conclusions:

The average period of the 5 days' persistence of small spills seems more probable in real average environmental conditions because it corresponds better to the Zipf's statistical distribution (i.e. their adjustment coefficient a is closer to 1). There is also justification of this average persistence, which should also depend on the size of spill as a reflection of Richardson turbulent dispersion law $K \propto l^{4/3}$ where K is the turbulent diffusion coefficient and l is the average size of the spill (see Platonov, 2002).

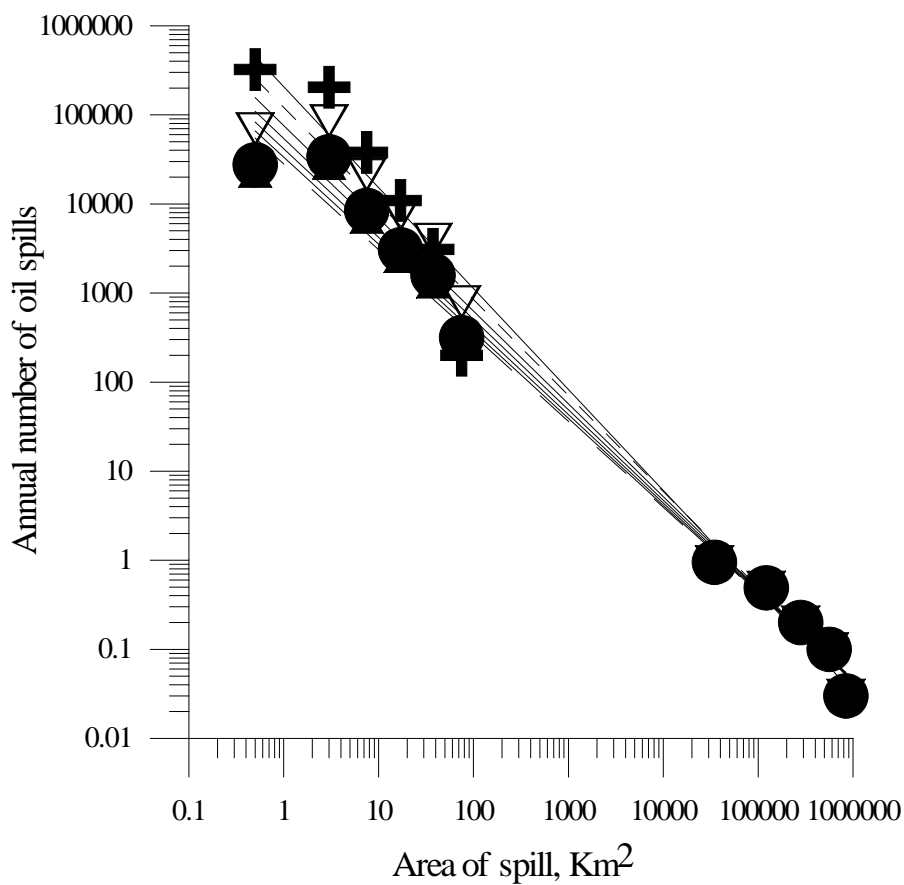


Figure Average annual number of small spills for different time periods of persistence in the sea surface together with the average annual number of great spills versus their respective areas. The mean number of the spills for the different persistence time periods are indicated by: ∇ - 2 days, - 3 days, - 4 days, \bullet - 5 days, - 6 days, Δ - 7 days, Different lines are the power fits according to the data of tables 3 and 4 Also plotted as + are the prediction of the number of small oil spills if the persistency is a function of the size and weather conditions.

References

M.O. Bezerra, M. Diez, C. Medeiros, A. Rodriguez, E. Bahia., A. Sanchez-Arcilla and J.M. Redondo (1998) Study on the influence of waves on coastal diffusion using image analysis. *Applied Scientific Research* 59,.191-204. 1998.

Linden P.F. and Redondo, J.M. (1991) Molecular mixing in RT instability, Part I, Global Mixing. *Physics of Fluids*,A 3, 1269-1277.

Matulka A., Redondo J.M. and Carrillo J.A.(2008) Experiments in stratified and rotating decaying 2D flows . *Il Nuovo Cimento C*, vol. 031, Issue 5, p.757-770.

Redondo J.M. and Garzon G. (2004) Multifractal structure and intermittent mixing in Rayleigh-Taylor driven fronts IWPCTM9.http://www.damtp.cam.ac.uk/proceedings/IWPCTM9/Papers/Redondo_Garzon/Talk.pdf

Mahjoub O., Redondo J.M. and Babiano A. (1998) Structure Functions in Complex Flows, *Applied Scientific Research* 59, 299-313.

Fraunie P., Berreba S. Chashechkin Y., Velasco D. and Redondo J.M. (2008) LES and laboratory experiments on the decay of grid wakes in strongly stratified flows. *Il Nuovo Cimento C* 31, 909-930.

Diez M., Bezerra M.O., Mosso C., Castilla R. and Redondo J.M. (2008) Experimental measurements and diffusion in coastal zones. *Il Nuovo Cimento C* 31,843-859.

Huq, P., Louis A. White, A. Carrillo, J.M. Redondo, S. Dharmavaram, S. R. Hanna, (2007): The Shear Layer above and in Urban Canopies. *J. Appl. Meteor. Climatol.*, **46**, 368–376. doi: 10.1175/JAM2469.1

Hurst, D., Vassilicos, J.C.(2007) Scalings and decay of fractal-generated turbulence. *Phys. Fluids* **19**, 035103, 2007.

Ishihara, T., Gotoh, T., Kaneda, Y.(2009) Study of high Reynolds number isotropic turbulence by direct numerical simulation. *Annu. Rev. Fluid Mech.* **41**, 165–180, 2009.

Laizet, S., Lamballais, E.(2009) High-order compact schemes for incompressible flows: a simple and efficient method with the quasi-spectral accuracy. *J. Comput. Phys.* **228**(16), 5989–6015, 2009.

Laizet, S., Lamballais, E., Vassilicos, J.C.(2010) A numerical strategy to combine high-order schemes, complex geometry and parallel computing for high resolution dns of fractal generated turbulence. *Comput. Fluids* **39**(3), 471–484. 2010.

Redondo, J.M. (2003) Topological Structures in Rotating Stratified Flows. *Topical Problems of Fluid Mechanics* eds: J. Prihoda, K. Kozel. Prague.

Redondo, J.M. and Linden, P.F.(1996) Geometrical observations of turbulent density interfaces. *The mathematics of deforming surfaces, IMA Series.* eds.D.G. Dritschel and R.J. Perkins Oxford: Clarendon Press Oxford. P. 221-248.

Redondo J.M. Grau J., Platonov A. and Garzon G. (2008) Analisis multifractal de procesos autosimilares: imagenes de satelite e inestabilidades baroclinas *Rev. Int. Met. Num. Calc. Dis. Ing.* Vol. 24, 1, 25-48 .2008.

